Longitudinal Tracking of Adiposity in a Canine Model of Insulin Resistance

E. B. Welch[1,2], J. Berglund[3], J. Kullberg[3], K. C. Coate[4], P. Williams[4], A. Cherrington[4], and M. J. Avison[1,2]
[1]Vanderbilt University Institute of Imaging Science, Vanderbilt University, Nashville, TN, United States, [2]Department of Radiology and Radiological Sciences, Vanderbilt University, Nashville, TN, United States, [3]Department of Radiology, Uppsala University, Uppsala, Sweden, [4]Department of Molecular Physiology and Biophysics, Vanderbilt University, Nashville, TN, United States

Introduction: The explosion in metabolic diseases, particularly insulin resistance and Type 2 diabetes mellitus (T2DM), driven by the obesity epidemic, has intensified the need for well-characterized animal models. Models in which whole body adiposity can be manipulated and the size of specific adipose tissue (AT) depots measured longitudinally and non-invasively, can help improve our understanding of the role of specific AT depots in the pathogenesis of obesity-associated metabolic diseases. Whole-body MRI is increasingly widely used to measure AT distribution in human subject research [1-5], but remains relatively under-utilized in translational large animal models. In this abstract, we describe the adaptation of a whole-body fat-water imaging (FWI) MRI acquisition and automated analysis pipeline, initially validated in human volunteers, for whole-body FWI in dogs. We demonstrate the utility of this pipeline by following the changes in lean and AT volume in dogs placed on an obesogenic high-fat, high-fructose diet known to increase insulin resistance [6], and comparing these changes with the observed change in body weight.

Methods: Dogs were scanned on a whole-body 3T Achieva scanner (Philips Healthcare, Best, The Netherlands) equipped with a Quasar Dual gradient set capable of 40 mT/m peak strength and 200 mT/m/ms peak slew rate. Animals were anesthetized, intubated and mechanically ventilated throughout the scanning session. All procedures were approved by the Vanderbilt IACUC. Animals entered the scanner feet-first in a supine position. A multi-station protocol with 12 table positions (stacks) was used to acquire the whole-body data, using the integrated quadrature body coil (QBC) for transmit and receive. Each stack consisted of a multi-slice, multi-echo gradient echo (multiple fast field echo: mFFE), acquisition with 20 contiguous 5mm slices; TR/TE1/TE2/TE3 [ms] = 150/1.34/2.87/4.40; FA=20º; WFS=0.251 pixels (BW=1734 Hz/pixel); FOV = 420 mm × 322 mm, acquired matrix size = 232 × 179; acquired voxel size = 1.8 mm × 1.8 mm× 5 mm. First order ("auto") shimming was performed for each slice stack. Flyback gradients were employed between echoes to maintain the same chemical shift direction for all echo readouts. The total duration of data acquisition was 5 minutes and 33 seconds. However, additional time was needed for the table movement, preparation phases at each table position, and for breath holding pauses. Breath holds (27.8 s) were applied for table positions sensitive to respiratory motion (pelvis to rib cage; typically 4 stations) by pausing the respirator. The normal phase correction algorithm applied by the scanner's reconstructor was disabled to allow for proper separation of the fat and water signals. Water and fat images were reconstructed by a custom in-line tool on the scanner console using a generalized three-point Dixon approach [4]. Whole-body fat free mass (FFM), whole-body fat mass (FM) and visceral adipose tissue (VAT) mass were determined using an automated segmentation and quantification pipeline previously used on human data [5], and adapted for dogs. Tissue volumes were converted to mass using densities of 0.923 kg/L for fatty tissue and 1.100 kg/L for lean tissue [7].

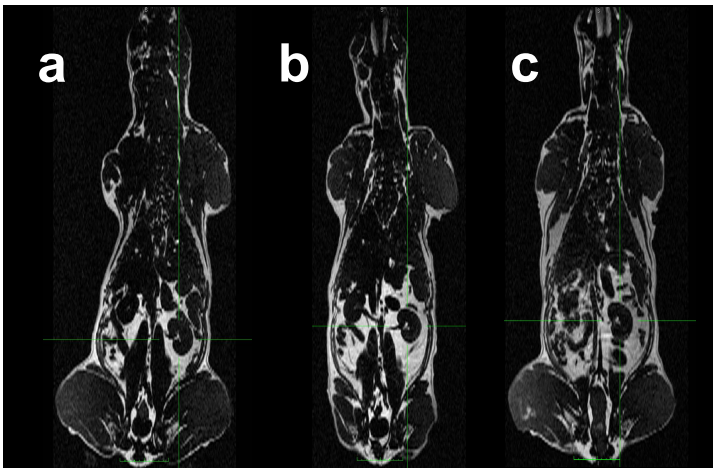

Figure 1. In vivo coronal fat images of a study dog imaged at baseline (0 weeks), and after 2 and 4 weeks on an obesogenic high-fat, high-fructose diet.

Weeks on Diet	0	2	4
Scale Mass [kg]	31.4	32.8	33.4
MRI Total Fat Free Mass [kg]	22.8	22.4	23.0
MRI Total Fat Mass [kg]	6.7	8.1	8.5
MRI VAT Mass [kg]	1.6	2.2	2.3

Table 1. Mass in kilograms for the canine subject at the 3 observed time points 0 (baseline), 2 and 4 weeks on diet as measured by a scale and by MRI. To obtain MRI masses, volumes were multiplied by literature tissue densities values for fat free mass (FFM) and fat mass (FM).

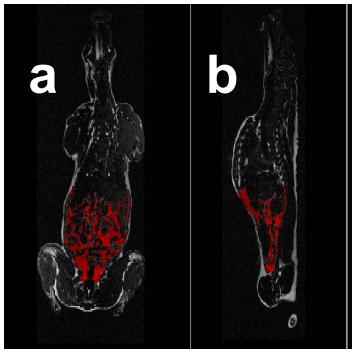

Figure 2. Coronal (**a**) and sagittal (**b**) sections displaying those voxels classified as visceral adipose tissue (red) by the automated segmentation pipeline.

Results: Figure 1 shows fat images collected from the same dog immediately before, and after two and four weeks of high-fat, high-fructose feeding. After just 2 weeks on the diet, the amount of visceral adipose tissue noticeably increased. Figure 2 shows an example of semi-automated VAT segmentation. The automated segmentation and quantification of the data from the dog in Figure 1 confirmed a close correspondence between the increase in Total Fat Mass and the measured weight gains at weeks 2 and 4, with little change in Total Fat Free mass (Table 1). A consistent shortfall in total calculated mass compared with the total weighed mass was observed and probably arises from a combination of incomplete coverage of the whole body, small errors in boundary classifications, and failure to account for different densities of different non-fat tissues, such as bone. Finally, while VAT comprised 23% of Total Fat Mass, the increase in VAT Mass accounted for 43% (2 weeks) and 39% (4 weeks) of the increase in Total Fat Mass.

Discussion: This study demonstrates the utility of whole-body fat water imaging using a multi-station, multi-gradient-echo fat-water MR imaging sequence at 3T for translational studies requiring non-invasive monitoring of body composition. The ability of FWMRI to quantify and localize body composition changes with respect to both lean and adipose tissue depots will provide a unique tool with which to examine the role of specific adipose tissue depots, and adiposity phenoytpes in the development of metabolic disease.

References: 1. Thomas EL et al. JAP (1998) 85:1778-1785. 2. Börnert P et al. JMRI (2007) 25:660-65. 3. Liu CY et al. MRM (2007) 58:354-364. 4. Berglund J et al. MRM (2010) 63(6):1659-1668. 5. Kullberg J et al. JMRI (2009) 30(1):185-193. 6. Coate KC et al. AJP (2010). 7. Chowdhury et al. IJORMD (1994).